



Available online at www.sciencedirect.com

SCIENCE @ DIRECT®

C. R. Chimie 8 (2005) 1353–1364



<http://france.elsevier.com/direct/CRAS2C/>

Account / Revue

Bridging diimino and ene-diamido ligands in binuclear compounds: structural and electronic features

Agustín Galindo

Departamento de Química Inorgánica, Universidad de Sevilla Aptdo. 553, 41701 Sevilla, Spain

Received 19 April 2004; accepted 21 July 2004

Available online 21 April 2005

Dedicated to Professor Carlo Mealli

Abstract

The structural and electronic features of bridging diimino and ene-diamido ligands in binuclear complexes are analyzed by means of the DFT approach. Three coordination modes are identified for these bridges. For each structural type their geometrical parameters and bonding properties are studied through the use of selected model compounds. **To cite this article:** A. Galindo, *C. R. Chimie 8 (2005)*.

© 2005 Académie des sciences. Published by Elsevier SAS. All rights reserved.

Résumé

Les propriétés structurelles et électroniques des ligands ponts type diimino et ène-diamidure dans les complexes binucléaires sont analysés selon l'approche DFT. Trois modes de coordination sont identifiés pour ces deux ligands pont. Pour chaque type de structure, nous utiliserons des modèles sélectionnés pour l'étude des paramètres géométriques et des propriétés de liaison. **Pour citer cet article :** A. Galindo, *C. R. Chimie 8 (2005)*.

© 2005 Académie des sciences. Published by Elsevier SAS. All rights reserved.

Keywords: Ene-diamido; Diimino; Binuclear compounds; DFT

Mots clés : Ene-diamidure ; Diimino ; Complexes binucléaires ; DFT

1. Introduction

In the last few years we have been interested in the theoretical analysis of transition metal compounds containing *o*-phenylenediamido ligands or, in general, ene-diamido ligands. Initially, we paid attention to the

bonding capabilities of the dianionic ene-diamido functionality that coordinates metals with a formal d^0 electron configuration [1]. The reasons that favor the observed folded 2,5-diazacyclopent-3-ene metallacycle were investigated in a number of Group 5 [2,3] and Group 4 derivatives [4]. Concerning the *o*-phenylenediamido ligand, their complexes with Group 6 metals in different oxidation states, were stud-

E-mail address: galindo@us.es (A. Galindo).

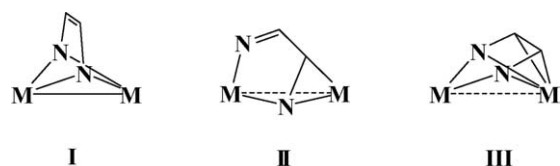


Fig. 1. Schematic representation of the three different coordination modes of bridging 1,4-diaza-1,3-butadiene skeleton in binuclear compounds. Substituents at N and C atoms are not shown.

ied from the structural and electronic points of view [5]. The *o*-phenylenediamido/*o*-diiminobenzene dichotomy of this non-innocent ligand was investigated as well in some mononuclear Group-8 derivatives [6].

In the last decade, the number of theoretical papers dedicated to the investigation of mononuclear species containing ene-diamido or diimino ligands have increased markedly [7–16]. Today, the number of theoretical studies devoted to binuclear systems with a bridging diimino ligand is still limited [17], although the chemistry of binuclear species containing bridging diimino ligands was initiated and developed several years ago by Vrieze and coworkers [18,19]. We have recently shown that the oxidation of binuclear ruthenium complexes of this type affects mainly the bridge and transforms the *o*-phenylenediamido ligand into a *o*-diiminobenzene one. The experimental results were justified by DFT calculations [20]. As a logical expansion of this work, this paper presents an overview of the different coordination modes found in known binuclear transition metal compounds, which contain bridging diimino or ene-diamido ligands. The electronic structures of the corresponding bridging ligands are analyzed and discussed in terms of the results of DFT calculations.

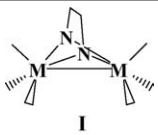
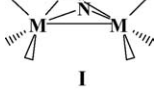



2. Results and discussion

2.1. Structural arrangements of ene-diamido and diimino ligands in binuclear compounds

We have centered our attention on structurally characterized compounds that contain the ene-diamido or the diimino fragments as a bridge between two metal atoms. Clusters of higher nuclearity are not considered in this paper [21–24]. From a search in the Cambridge Structural Database [25] three different coordination modes are identified (see Fig. 1). They are, respectively, μ - η^2 -(N, N'), η^2 -(N, N'), **I**, μ - η^2 -(N, N'), η^2 -(N, C), **II**, and μ - η^2 -(N, N'), η^4 -(N, N', C, C'), **III**. The bridging ligand in the coordination modes **I** and **III** behaves as a eight electron donor. However, in **I** the bridge has the dianionic ene-diamido character, while in mode **III** displays a neutral diimino nature. In the latter coordination mode, two nitrogen σ lone pairs and two π contributions of C=N bonds are donated to each metal respectively. Finally, the ligand in **II** is also neutral and behaves as a six electron donor. Four electrons are donated to one metal through the nitrogen σ combinations of diimino, whereas the third pair of electrons come from the π contribution of one C=N bond and are donated to the second metal (Fig. 1).

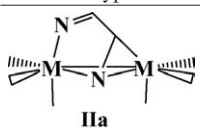
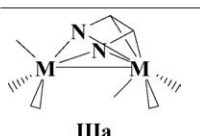
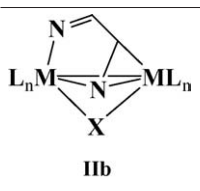
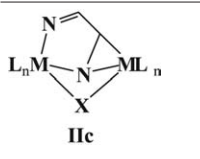
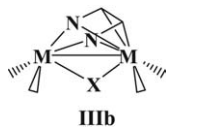
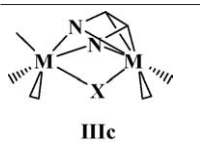
On the basis of the structural features, the complexes may be distinguished in seven different categories. Tables 1 and 2 show a simplified scheme for each structural type, the complex formula and the corresponding CCDC refcode. Table 1 displays the examples in which the bridging ligand is of $C_6H_4(NR)_2$ -*o* type, whereas Table 2 shows those in which the bridge does not contain the aryllic backbone.

Table 1
Structural arrangements of the $C_6H_4(NR)_2$ -*o* ligand in binuclear compounds^a

Structural types	Formula	Refcode and reference
	$[Ru_2\{\mu-C_6H_4(NH)_2-o\}(CO)_4(PPh_3)_2]$	JETPED, JETPIH [26]
	$[Fe_2\{\mu-C_6H_4(NH)(NPh)-o\}(CO)_6]$	SEMFEC10 [27]
	$[Fe_2\{\mu-C_6H_4(NH)(N^tBu)-o\}(CO)_6]$	SIYXED [28]
	$[Ru_2\{\mu-C_6H_4(NH)_2-o\}(\mu-dppm)(CO)_2(PPh_3)_2]$	SOQCUM [29]
	$[Ru_2\{\mu-C_6H_4(NH)_2-o\}(\mu-dppm)(CO)_2(PPh_3)_2](PF_6)_2]$	AROQAZ [20]

^a The phenylene ring is not drawn in the charts.

Table 2
Structural arrangements of the R,R'-DAD diimino ligand in binuclear compounds^a

Structural types	Formula	Refcode and reference
 IIa	[Fe ₂ (μ- <i>p</i> -C ₆ H ₄ Me, OCH ₂ CH(CH ₂) ₃ N-DAD)(CO) ₆]	CUQLAB [30]
	[Fe ₂ (μ- <i>p</i> -C ₆ H ₄ OMe, OCH ₂ CH(CH ₂) ₃ N-DAD)(CO) ₆]	CUQLEF [30]
	[(CO) ₃ Ru(μ- ^{<i>i</i>} Pr, H-DAD)Fe(CO) ₃]	GIFXIC [31]
	[Fe ₂ (μ-Cy, H-DAD)(CO) ₆]	HXBCFE [32]
 IIIa	[Mn ₂ (μ-Ph, Ph-DAD)(CO) ₆]	JAPTEZ [33]
	[Mn ₂ (μ-Me, Me-DAD)(CO) ₆]	MEAZMN [34]
	[Mn ₂ (μ- <i>p</i> -C ₆ H ₄ Me, <i>p</i> -CH ₂ C ₆ H ₄ Cl-DAD)(CO) ₆]	MNCLPD10 [33]
 IIb	[Ru ₂ (μ- ^{<i>i</i>} Pr, H-DAD) ₂ (CO) ₄]	COGXRU [35]
	[CpRu(μ- ^{<i>i</i>} Bu, H-DAD)(μ-CO)Co(CO) ₂]	GIFXUO [36]
	[(CO) ₃ Mn(μ- ^{<i>i</i>} Bu, H-DAD)(μ-CO)Co(CO) ₂]	GXCOMN [37]
	[(CO) ₂ ClRu(μ- ^{<i>i</i>} Pr, H-DAD)(μ-H)Ru(CO) ₃]	WAGKOE [38]
 IIc	[(CO) ₂ MeRu(μ- ^{<i>i</i>} Pr, H-DAD)(μ-I)Ru(CO) ₂ (PMe ₂ Ph)]	YAJXOW [39]
 IIIb	[Ru ₂ (μ- ^{<i>i</i>} Pr, H-DAD)(μ-CO)(CO) ₄]	CIYRAD [40]
	[Ru ₂ (μ- ^{<i>i</i>} Pr, H-DAD)(μ-HCCH)(CO) ₄]	GLXRUA10 [41]
	[Fe ₂ (μ- ^{<i>i</i>} Pr, H-DAD)(μ-HCCOOMe)(CO) ₄]	JANFEJ [42]
 IIIc	[(CO) ₃ Ru(μ- ^{<i>i</i>} Pr, H-DAD)(μ-CCOOMe)Fe(CO) ₂]	SASYAM [43]
	[(CO) ₂ MeRu(μ- ^{<i>i</i>} Pr, H-DAD)(μ-I)Ru(CO) ₂]	YAJXEM [39]

^a R,R'-DAD represents the substituted 1,4-diaza-1,3-butadiene RN=CR'CR'=NR.

The general arrangements of the bridging ligand, displayed in Fig. 1, are encountered in both Tables 1 and 2, although with some sub-distinctions. In **I** the ligand bridges the two metals through the N atoms and maintains its molecular plane perpendicular to the M–M bond (μ-η²-(N, N'), η²-(N, N') bonding type). In mode **IIa** the diazabutadiene ligand binds one metal through the N=C bond, while the second metal atom is coordinated by both nitrogen atoms (μ-η²-(N, N'), η²-(N, C) bonding type). The modes **IIb** and **IIc**, which differ for the presence or absence of M–M bond, are similar to

that of **IIa** but the diazabutadiene bridge is not unique, but there is an additional bridge X. The latter coordinates both metals through a single atom (e.g., CO, H or halide) or two linked atoms (e.g. acetylene type ligand). Alternatively, the additional bridge is a second diazabutadiene ligand. In mode **IIIa** the diazabutadiene molecule is bent towards one metal atom and the short M–C contacts are indicative of a bonding interaction. Again, types **IIIb** and **IIIc** feature the same coordination mode of **IIIa**, μ-η²-(N, N'), η⁴-(N, N', C, C'), and have an additional bridging ligand X. Their main difference is

the presence or absence of a direct metal–metal bond, respectively.

In order to gain a general overview of the structural and electronic features of the coordinated 1,4-diaza-1,3-butadiene skeleton in these binuclear complexes, representative models for each subclass were selected and theoretical calculations were carried out followed by a bonding analysis.

2.2. Ene-diamido $\mu\text{-}\eta^2\text{-(N, N')}, \eta^2\text{-(N, N')}$ bridging ligand

Recently, the MO distribution of $[\text{Ru}_2\{\mu\text{-C}_6\text{H}_4(\text{NH})_2\text{-}o\}(\mu\text{-dppm})(\text{CO})_2(\text{PPh}_3)_2]$ complex, in which the *o*-phenylenediamido ligand symmetrically bridges the two metal atoms ($\mu\text{-}\eta^2\text{-(N, N')}, \eta^2\text{-(N, N')}$, type I), has been analyzed by DFT methods [20]. Model compound $[\text{Ru}_2\{\mu\text{-C}_6\text{H}_4(\text{NH})_2\text{-}o\}(\mu\text{-H}_2\text{PCH}_2\text{PH}_2)(\text{PH}_3)_2(\text{CO})_2]$ has been adopted and the bonding scheme, previously discussed by EHMO method [44] has been consistently confirmed. Curiously enough, from the inspection of Tables 1 and 2 one can see that the $\mu\text{-}\eta^2\text{-(N, N')}, \eta^2\text{-(N, N')}$ arrangement is specific for *o*-phenylenediamido ligand and not for structurally characterized examples containing the 1,4-diaza-1,3-butadiene ligand (that is, without the aryl backbone). In fact, the ligands of type R,R'-DAD adopt the bridging coordination modes II or III exclusively.

In order to gain further information about the bonding capabilities of the *o*-phenylenediamido ligand, calculations on the simplest model compounds $[\text{M}_2\{\mu\text{-C}_6\text{H}_4(\text{NH})_2\text{-}o\}(\text{CO})_6]$ ($\text{M} = \text{Fe}$, **1a**; Ru , **2a**) were performed with the coordination mode $\mu\text{-}\eta^2\text{-(N, N')}, \eta^2\text{-}$

(N, N'), I. The optimized structure of the iron derivative **1a** is displayed in Fig. 2, while its computed structural parameters are reported in Table 3. A good correlation with the experimental values of the $[\text{Fe}_2\{\mu\text{-C}_6\text{H}_4(\text{NH})(\text{NR})\text{-}o\}(\text{CO})_6]$ complexes was found. The calculated C–C and N–C lengths are in agreement with a dianionic ene-diamido character of the $\text{C}_6\text{H}_4(\text{NH})_2\text{-}o$ ligand. Also, the results for **2a** are consistent with the geometry of the $[\text{Ru}_2\{\mu\text{-C}_6\text{H}_4(\text{NH})_2\text{-}o\}(\text{PPh}_3)_2(\text{CO})_4]$ complex (see Section 5). For both, **1a** and **2a** derivatives, the MO analysis previously reported for *o*-phenylenediamido ruthenium complexes of type I is well suited and does not require further comment. The computed HOMO for the model **1a** comes from interaction of the filled π_3^* orbital with the $1b_1$ metal combination and is largely ligand centered, whereas HOMO-1 accounts for the direct Fe–Fe interaction. The computed charges of both iron atoms are 1.27 and the Fe–Fe interaction is a non-polarized metal–metal bond in a $d^7\text{-}d^7$ $\text{L}_3\text{M-ML}_3$ system.

The ruthenium derivative $[\text{Ru}_2(\text{DAD})(\text{CO})_6]$, **2b**, (DAD = HNCCHNH) was previously optimized [20]. The suitable results obtained after simplification of the *o*-phenylenediamido group by DAD ligand prompted us to optimize as well the simplest model compound $[\text{Fe}_2(\text{DAD})(\text{CO})_6]$, **1b**, with the DAD ligand arranged as in I and without symmetry constraints. The resulting structure of **1b** is shown in Fig. 3. The computed structural parameters are close to those of **1a** and are also collected in Table 3 for the appropriate comparison. No noteworthy differences can be observed after the oversimplification of the *o*-phenylenediamido ligand (dismissal of the aryl backbone).

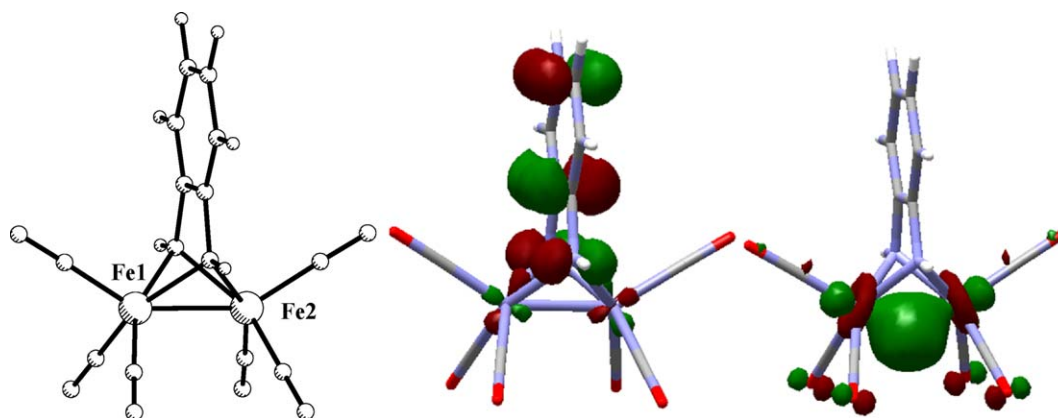
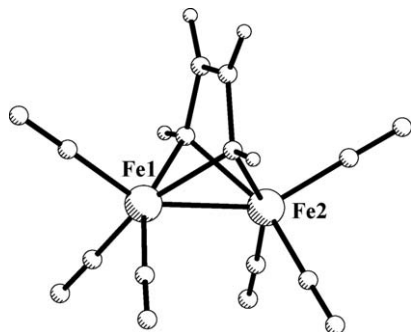
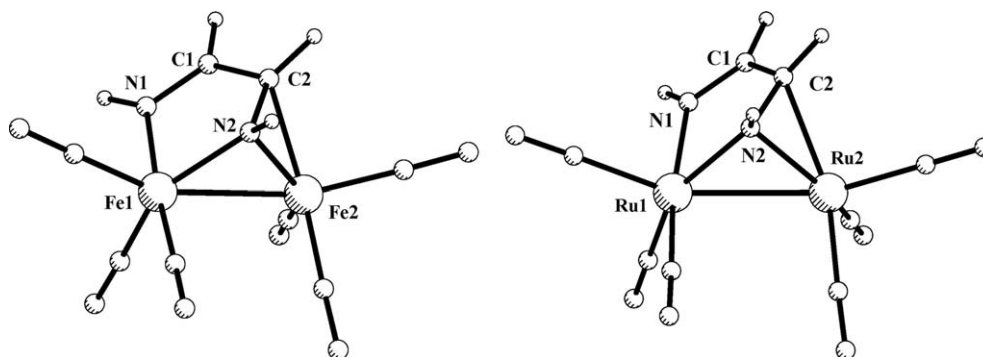


Fig. 2. Optimized structure of model compound $[\text{Fe}_2\{\text{C}_6\text{H}_4(\text{NH})_2\text{-}o\}(\text{CO})_6]$, **1a**, and its HOMO and HOMO-1 orbitals.

Table 3

Selected structural parameters of calculated iron complexes $[\text{Fe}_2\{\text{C}_6\text{H}_4(\text{NH})_2\text{-}o\}(\text{CO})_6]$, **1a**, and $[\text{Fe}_2(\text{DAD})(\text{CO})_6]$, **1b**, (coordination mode I) and comparison with experimental data

Bond distances (Å) and angles (°)	Calculated		Experimental, $[\text{Fe}_2\{\mu\text{-C}_6\text{H}_4(\text{NH})(\text{NR})\text{-}o\}(\text{CO})_6]$	
	1a	1b	R = Ph, SEMFEC10	R = ^t Bu, SIYXED
Fe1–Fe2	2.367	2.361	2.37	2.384(1)
Fe1–N	2.014	2.021	1.98	1.963(5)
			2.02	2.066(5)
Fe2–N	2.014	2.021	2.00	1.963(6)
			2.02	2.062(5)
N–C	1.423	1.433	1.44	1.421(7)
			1.45	1.476(7)
C–C	1.408	1.339	1.36	1.38
Fe1–CO(up)	1.806	1.805	1.80	1.822(8)
Fe2–CO(up)	1.806	1.805	1.82	1.807(8)
Fe1–CO(down)	1.796	1.796	1.78	1.756(7)
			1.78	1.763(8)
Fe2–CO(down)	1.796	1.796	1.76	1.755(8)
			1.77	1.787(8)
C–C–N	109.7	110.6	109.8	109.6(5)
			111.4	111.0(6)
Fe2–Fe1–CO(up)	148.3	148.1	146.9	147.2(3)
			149.3	147.5(2)

Fig. 3. Optimized structure of **1b**.Fig. 4. Optimized structures of compounds $[\text{M}_2(\text{DAD})(\text{CO})_6]$ ($\text{M} = \text{Fe}$, **1c**; Ru , **2c**).

2.3. Diimino $\mu\text{-}\eta^2\text{-(N, N')}, \eta^2\text{-(N, C)}$ bridging ligand

Concerning the coordination mode $\mu\text{-}\eta^2\text{-(N, N')}, \eta^2\text{-(N, C)}$ (type **II**), the model compounds $[\text{M}_2(\text{DAD})(\text{CO})_6]$ ($\text{M} = \text{Fe}$, **1c**; Ru , **2c**) were optimized without symmetry restrictions. The resulting structures are displayed in Fig. 4. The computed structural parameters for the iron derivative **1c** are grouped in Table 4. Bond distances and angles show a reasonable agreement when compared with those found experimentally. The calculated N–C bonds are characterized by two different distances of 1.299 and 1.405 Å, N1–C1 and N2–C2, respectively. The former distance is close to that of a

Table 4

Selected structural parameters of calculated $[\text{Fe}_2(\text{DAD})(\text{CO})_6]$ complex, **1c**, (coordination mode **II**) and comparison with experimental data

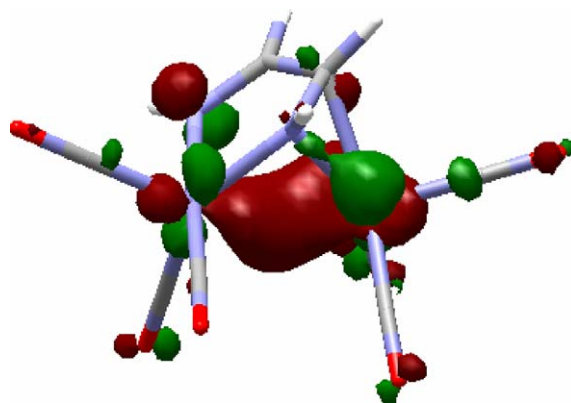
Bond distances (Å) and angles (°)	Calculated 1c	Experimental		
		HXBCFE	CUQLAB	CUQLEF
Fe1–Fe2	2.628	2.60	2.565(1)	2.592(9)
Fe1–N1	2.004	1.97	2.015(6)	2.015(4)
Fe1–N2	1.962	1.99	1.959(6)	1.968(4)
Fe2–N2	1.915	1.93	1.926(6)	1.929(4)
Fe2–C2	2.098	2.07	2.021(6)	2.045(5)
N1–C1	1.299	1.28	1.304(8)	1.313(6)
N2–C2	1.405	1.40	1.394(8)	1.397(6)
C1–C2	1.429	1.43	1.497(9)	1.495(6)
C–C–N	117.3	115.5	116.0(6)	116.4(4)
	115.0	118.6	112.3(6)	112.9(4)

typical double N=C bond, while the latter is slightly shorter than the computed NC bond in the ene-diamido complex **1a**. These values are in conformity with a diimino description of the diazabutadiene bridging ligand. Selected calculated bond lengths and angles of compound $[\text{Ru}_2(\text{DAD})(\text{CO})_6]$, **2c**, are only included as Supplementary Material because no structural data are available for comparison. However, it is important to highlight that the computed IR spectrum of **2c** in the $\nu(\text{CO})$ region (2054, 2012, 1992, 1983, 1958 and 1956 cm^{-1}) fits quite well with the reported IR spectra of $[\text{Ru}_2(\text{R,R}'\text{-DAD})(\text{CO})_6]$ complexes [35].

The bridging diimino ligand in these $[\text{M}_2(\text{DAD})(\text{CO})_6]$ complexes behaves as a six electron donor to the $d^8\text{-}d^8 \text{ L}_3\text{M-ML}_3$ system, behaving the dihapto bonded C=N bond as the equivalent of a two electron donor. Each metal displays pseudo-octahedral and trigonal bipyramidal coordination environments at the atoms Fe1 and Fe2, respectively (see **1c**, Fig. 4). As a possible interpretation, the metal–metal bond can be considered of dative nature. According to the latter, the metal–metal interaction stems from the donation of a filled $\sigma\text{-ML}_5$ hybrid onto an empty $\sigma\text{-ML}_4$ one. The calculated HOMO for **1c**, shown in Fig. 5, supports the viewpoint. The computed metal charges (0.41 and 0.12 for the Fe1 and Fe2 atoms in **1c**, respectively) account well for the presence of a polarized metal–metal bond.

2.4. Comparison of the coordination modes $\mu\text{-}\eta^2\text{-(N, N')}, \eta^2\text{-(N, N')}$, type **I**, and $\mu\text{-}\eta^2\text{-(N, N')}, \eta^2\text{-(N, C)}$, type **II**, in compounds with the same general formulation $[\text{M}_2(\text{DAD})(\text{CO})_6]$ ($M = \text{Fe, Ru}$)

The optimizations of iron and ruthenium binuclear complexes with similar formulation $[\text{M}_2(\text{DAD})(\text{CO})_6]$

Fig. 5. HOMO of **1c**.

and different coordination modes $\mu\text{-}\eta^2\text{-(N, N')}, \eta^2\text{-(N, N')}$, **I**, and $\mu\text{-}\eta^2\text{-(N, N')}, \eta^2\text{-(N, C)}$, **II**, computed at the same level of theory, allow us to adequately compare their structural and energetic features (**1b** vs. **1c** and **2b** vs. **2c**). Regarding the bond distances, the C–C bond length of the metallacycle is longer in compounds **1c** and **2c** (diimino $\mu\text{-}\eta^2\text{-(N, N')}, \eta^2\text{-(N, C)}$, coordination mode **II**) than the same value in **1b** and **2b** (for example, 1.429 versus 1.339 Å for $M = \text{Fe}$), in agreement with the ene-diamido formulation of the bridge (mode **I**) in the latter complexes. Additionally, both C–N distances in the complexes of type **c** (diimino) are shorter than those found for **b** complexes (for example, 1.299 and 1.405 versus 1.433 Å for $M = \text{Fe}$). These structural differences accompany also to different formal charges of the metal atoms. Comparison of the iron charges in compounds **1b** (0.79 for the two atoms) and **1c** (0.41 and 0.12 for the Fe1 and Fe2 atoms, respectively) confirms the different formulation of the bridge.

Concerning the energies, the $[\text{M}_2(\text{DAD})(\text{CO})_6]$ isomers of type **c** are found to be slightly more stable than

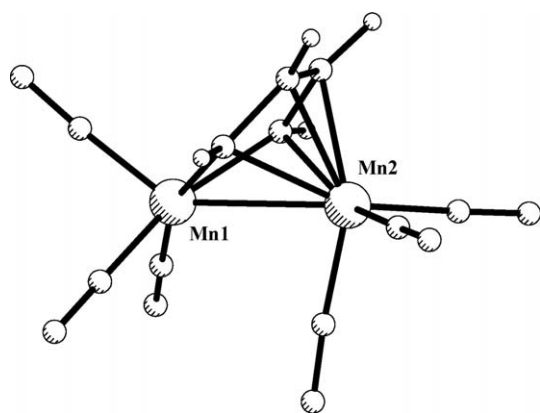


Fig. 6. Optimized structure of model compound $[\text{Mn}_2(\text{DAD})(\text{CO})_6]$, **3**.

those of type **b**. The energy differences are computed to be 2.5 and 3.0 kcal mol⁻¹, for M = Fe and Ru, respectively. This fact suggests that the $\mu\text{-}\eta^2\text{-(N, N')}, \eta^2\text{-(N, C)}$ coordination mode for the 1,4-diaza-1,3-butadiene ligand is slightly privileged with respect to the $\mu\text{-}\eta^2\text{-(N, N')}, \eta^2\text{-(N, N')}$ one. However, when the bridging ligand contains the *o*-phenylenediamido group the structural situation is that represented by **I**, according to the experimental evidence. A plausible explanation for this fact is the following: generally, the H–C–C–H (or R'–C–C–R') torsion angle of coordinated diimine ligands are close to 0°. However, the computed H–C–C–H torsion angle for DAD in the complexes **1c** and **2c** is ca. 17°, a value that is not compatible with the planar *o*-phenylene backbone.

2.5. $\mu\text{-}\eta^2\text{-(N, N')}, \eta^4\text{-(N, N', C, C')}$ bridging ligand

The chemical oxidation of $[\text{Ru}_2\{\mu\text{-C}_6\text{H}_4(\text{NH})_2\text{-}o\}(\mu\text{-dppm})(\text{CO})_2(\text{PPh}_3)_2]$ complex affords $[\text{Ru}_2\{\mu\text{-C}_6\text{H}_4(\text{NH})_2\text{-}o\}(\mu\text{-dppm})(\text{CO})_2(\text{PPh}_3)_2](\text{PF}_6)_2$, in which the $\text{C}_6\text{H}_4(\text{NH})_2\text{-}o$ ligand adopts the $\mu\text{-}\eta^2\text{-(N, N')}, \eta^4\text{-(N, N', C, C')}$ coordination mode (**III**) and behaves as an eight-electron donor in the diimino form. The structural characterization of the latter compound, together with a theoretical analysis of the simplest model compound $[\text{Mn}_2(\text{DAD})(\text{CO})_6]^{2+}$, has recently appeared [20]. In order to generalize the attributes of the bonding mode **III**, the formally isoelectronic model compound $[\text{Mn}_2(\text{DAD})(\text{CO})_6]$, **3**, has also been studied for a convenient comparison. The optimized geometry of **3** is depicted in Fig. 6. Table 5 shows selected structural data (experimental and calculated) corresponding to the

known $[\text{Mn}_2(\text{R,R}'\text{-DAD})(\text{CO})_6]$ complexes. In general, there is a satisfactory agreement between the calculated and experimental geometric parameters, the bond distances agree within 0.05 Å, except for the Mn–Mn separation. Although the latter is clearly overestimated, its value of 2.723 Å is still consistent with a direct metal–metal bond [45]. The C–C and N–C lengths of 1.399 and 1.379 Å, respectively, are in conformity with a diimino constitution of the DAD ligand.

The frontier MOs of the diimino DAD ligand include two filled σ lone pairs (in phase σ_{ip} and out phase σ_{op}) that correspond to the HOMO and HOMO-1 of the molecule; two filled, lower in energy, π_1 and π_2 combinations and two empty π^* combinations (π_3^* and π_4^*). Consequently, the bonding capabilities of this ligand arises from the two nitrogen σ lone pairs and the two filled π MOs, making possible the donation to the metals of eight electrons. On the basis of a FMO analysis, essentially, the qualitative picture of the bonding in **3** may be described as the ligand-to-metal donation of the two σ lone pairs to Mn1 atom and of the two π combinations to Mn2 atom. The different Mn1–N and Mn2–N distances accounts well with this explanation. Moreover, the specific orientation of the MnL_3 fragment at the atom Mn2 atom is well rationalized with the backdonation from one of the well known d_{π} metal hybrids (2e levels) of a $\text{C}_{3v}\text{-ML}_3$ fragment [46] into the empty π_3^* level of the bridging ligand.

The two-electron chemical oxidation of ruthenium complexes of type **I** determines the reorganization of the $\text{C}_6\text{H}_4(\text{NH})_2\text{-}o$ ligand to the structural type **III**. This experimental fact has been studied theoretically in the model compounds $[\text{Ru}_2(\text{DAD})(\text{CO})_6]$ and $[\text{Ru}_2(\text{DAD})(\text{CO})_6]^{2+}$. However, the removal of two electrons in the binuclear system may formally occur by the simple elimination of one ligand acting as 2e donor. For example, Vrieze and coworkers reported the dissociation of CO from $[\text{Ru}_2(\text{R,R}'\text{-DAD})(\text{CO})_6]$ complexes (coordination type **I**) to give $[\text{Ru}_2(\text{R,R}'\text{-DAD})(\mu\text{-CO})(\text{CO})_4]$ (coordination type **III**). Analogously, the same authors observed the formation of $[\text{Ru}_2(\text{R,R}'\text{-DAD})(\text{HCCH})(\text{CO})_4]$ compounds (coordination type **III**) by interaction of species $[\text{Ru}_2(\text{R,R}'\text{-DAD})(\text{CO})_6]$ with acetylene. Both types of compounds have been studied through the respective models $[\text{Ru}_2(\text{DAD})(\mu\text{-CO})(\text{CO})_4]$, **4**, and $[\text{Ru}_2(\text{DAD})(\mu\text{-HCCH})(\text{CO})_4]$, **5**. Full geometry optimizations were performed for **4** and **5** (both with imposed symmetry C_s) and the resulting

Table 5

Selected structural parameters of $[\text{Mn}_2(\text{R,R}'\text{-DAD})(\text{CO})_6]$ manganese complexes (coordination mode **III**) and comparison with experimental data

Bond distances (Å) and angles (°)	Calculated 3	Experimental		
		R = R' = Ph, JAPTEZ	R = <i>p</i> -C ₆ H ₄ -Me, R' = <i>p</i> -C ₆ H ₄ -Cl, MNCLPD10	R = R' = Me, MEAZMN
Mn1–Mn2	2.723	2.612(1)	2.633(1)	2.615(1)
Mn1–N	1.986	1.984(4)	1.962(5)	1.977(3)
		1.975(3)	1.958(5)	1.995(3)
Mn2–N	2.141	2.092(4)	2.087(5)	2.108(3)
		2.137(3)	2.084(5)	2.111(3)
Mn2–C	2.141	2.149(4)	2.131(6)	2.137(4)
		2.153(4)	2.124(6)	2.147(4)
N–C	1.379	1.387(5)	1.387(8)	1.392(5)
		1.397(5)	1.377(8)	1.388(5)
C–C	1.399	1.418(6)	1.397(8)	1.407(5)
Mn1–CO(up)	1.779	1.760(6)	1.748(8)	1.789(4)
Mn1–CO(down)	1.818	1.804(6)	1.809(7)	1.804(4)
		1.791(6)	1.811(8)	1.810(4)
Mn2–CO(up)	1.805	1.788(5)	1.803(7)	1.801(4)
		1.802(6)	1.804(7)	1.804(4)
Mn2–CO(down)	1.809	1.804(6)	1.811(7)	1.808(4)
C–C–N	112.3	111.3(4)	112.0(6)	112.3(3)
		111.8(4)	110.5(5)	112.7(3)
Mn1–Mn2–CO(down)	77.0	74.3(2)	75.5(2)	75.9(1)
Mn2–Mn1–CO(up)	143.5	148.8(2)	146.4(3)	148.5(1)

final geometries are shown in Fig. 7. Selected calculated parameters and, for comparison, selected experimental data from X-ray crystallography have been collected in Tables 6 and 7, respectively. The geometrical features of the diimino ligand in **4** and **5** are similar and adequately match the reported structures. Furthermore, the computed IR bands concerning the CO region (2029, 2000, 1964, 1958, 1848 cm^{-1} for **4** and 2020, 2001, 1958, 1956 cm^{-1} for **5**) correctly reproduce the experimental trends.

Both compounds were analyzed theoretically in an early work [17]. Our results are in agreement with the bonding description presented in that paper except for the proposed lack of the metal–metal bond. This fact may be re-interpreted on the basis of our results. At variance with complex **2c** in which the metal–metal interaction appears in the HOMO (see Fig. 5), an analogous level for complex **4** is found in the HOMO-7 and it is significantly delocalized (Fig. 8). Moreover, the higher filled MOs feature also some antibonding metal–

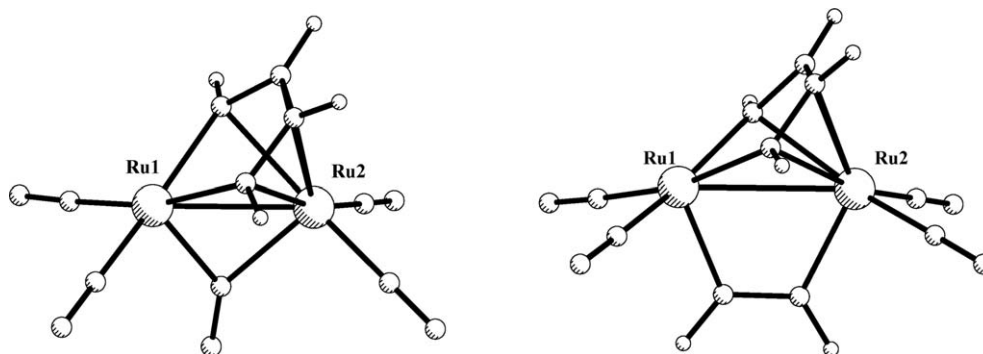
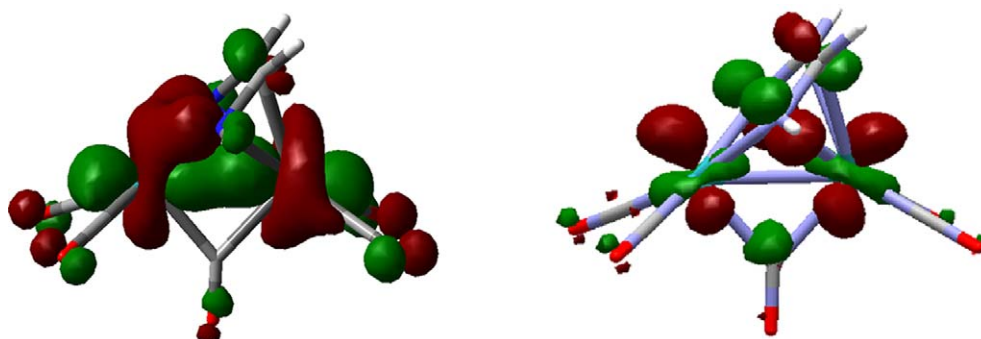


Fig. 7. Optimized structures of model compounds $[\text{Ru}_2(\text{DAD})(\mu\text{-CO})(\text{CO})_4]$, **4**, and $[\text{Ru}_2(\text{DAD})(\mu\text{-HCCH})(\text{CO})_4]$, **5**.

Fig. 8. HOMO-7 and LUMO of **4**.Table 6
Selected structural parameters of $[\text{Ru}_2(\text{R,R}'\text{-DAD})(\mu\text{-CO})(\text{CO})_4]$

Bond distances (Å) and angles (°)	Calculated R = R' = H, 4	Experimental R = ⁱ Pr, R' = H, CIYRAD
Ru–Ru	2.796	2.741(1)
Ru1–N	2.158	2.14(1) 2.14(1)
Ru2–N	2.319	2.27(1) 2.25(1)
Ru2–C	2.360	2.27(1) 2.28(1)
Ru1–C _{bridging}	2.063	2.03(1)
Ru2–C _{bridging}	2.121	2.15(1)
N–C	1.383	1.43(1) 1.43(1)
C–C	1.397	1.39(2)
Ru–N–Ru	77.2	76.7(3) 77.1(3)
C–C–N	114.4	115.9(9) 114.7(10)
Ru1–C–O _{bridging}	137.0	138.7(10)
Ru2–C–O _{bridging}	139.1	139.4(10)

metal character and determine the poor metal–metal overlap population, pointed out by the authors [17]. Metal–metal bonds are frequently difficult to investigate and new approaches are continuously emerging [47,48]. Although no additional deeper studies have been performed, on the basis of our results the existence of a metal–metal interaction in **4** is a conclusion preferable to that of its non-existence. In fact, the computed Ru–Ru bond length in **4** is slightly shorter than in **2c** (2.819 Å), where the Ru–Ru bond is not questionable.

The experimental evidence of CO dissociation in $[\text{Ru}_2(\text{R,R}'\text{-DAD})(\text{CO})_6]$ complexes has a theoretical confirmation from the present calculations. In **2c**, the

Table 7
Selected structural parameters of $[\text{Ru}_2(\text{R,R}'\text{-DAD})(\mu\text{-HCCH})(\text{CO})_4]$

Bond distances (Å) and angles (°)	Calculated R = R' = H, 5	Experimental R = ⁱ Pr, R' = H, GLXRUA10
Ru1–Ru2	3.049	2.936(1)
Ru1–N	2.139	2.117(6) 2.111(6)
Ru2–N	2.311	2.226(6) 2.225(6)
Ru2–C	2.295	2.226(7)
Ru1–C _{bridging}	2.065	2.062(9)
Ru2–C _{bridging}	2.093	2.092(8)
Ru1–CO	1.889	1.862(9) 1.844(9)
Ru2–CO	1.878	1.869(8) 1.864(8)
N–C	1.394	1.40(1) 1.451(9)
C–C (DAB)	1.396	1.396(11)
C–C (acetylene)	1.321	1.34(1)
Ru–N–Ru	86.4	84.2(2) 84.5(2)
C–C–N	113.9	116.4(7) 112.1(6)

dissociated CO molecule is precisely the ligand that displays the longest M–CO distance. The computed energy for the process represented in Eq. (1) is $-10.64 \text{ kcal mol}^{-1}$. This value agrees with the experimental observation of dissociation of CO upon refluxing the $[\text{Ru}_2(\text{R,R}'\text{-DAD})(\text{CO})_6]$ complexes in toluene [40]. The LUMO of **4** is characterized by a hybrid directed toward the created vacant position (see Fig. 8).

Finally, a representative example of the structures of type **IIIc** has been chosen. The model compound $[(\text{CO})_2\text{MeRu}(\mu\text{-DAD})(\mu\text{-I})\text{Ru}(\text{CO})_2]$, **6**, has been optimized with no symmetry constrains. Fig. 9 shows the

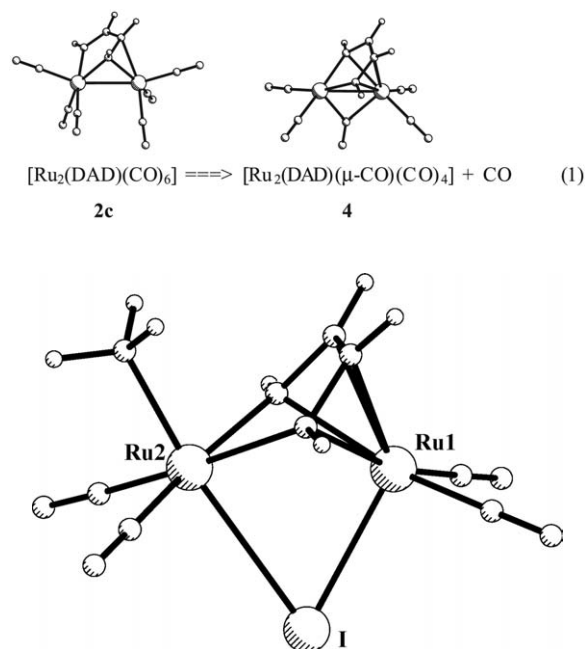


Fig. 9. Optimized structure of model compound $[(\text{CO})_2\text{MeRu}(\mu\text{-R,R}'\text{-DAD})(\mu\text{-I})\text{Ru}(\text{CO})_2]$, **6**.

Table 8
Selected structural parameters of $[(\text{CO})_2\text{MeRu}(\mu\text{-R,R}'\text{-DAD})(\mu\text{-I})\text{Ru}(\text{CO})_2]$

Bond distances (Å) and angles (°)	Calculated R = R' = H, 6	Experimental R = ⁱ Pr, R' = H, YAJXEM
Ru1–Ru2	3.150	3.0635(6)
Ru1–N	2.245	2.196(3) 2.197(3)
Ru2–N	2.180	2.150(4) 2.162(4)
Ru1–C	2.231	2.162(4) 2.160(5)
Ru2–CH ₃	2.121	2.115(5)
N–C	1.377	1.377(6) 1.366(6)
C–C	1.417	1.422(7)
Ru1–I	2.806	2.7517(5)
Ru2–I	3.172	3.0215(5)
Ru1–CO	1.899	1.870(5) 1.891(5)
Ru2–CO	1.887	1.856(5) 1.860(4)

resulting structure and Table 8 summarizes selected structural parameters and their comparison with the experimental data [39].

The calculated geometry of **6** is in good agreement with the experimental structure of complex $[(\text{CO})_2\text{MeRu}(\mu\text{-}^i\text{Pr,H-DAD})(\mu\text{-I})\text{Ru}(\text{CO})_2]$. In addition, the computed carbonyl IR bands (2030, 2017, 1977 and 1988 cm^{-1}) are in accord with the experimental values. Again, the bond distances support the diimino formulation of the DAD ligand, which behaves as a 8e donor. Thus, the complex features a $d^6\text{-RuL}_4$ fragment (at Ru2) saturated from the nitrogen σ lone pairs and a $d^8\text{-RuL}_3$ fragment (at Ru1) which is η^4 coordinated by the π system of DAD (four π electrons, donation and backdonation). No metal–metal bond exists in view of the long Ru–Ru distance (3.063 Å experimental and 3.150 Å computed).

3. Conclusions

The diazabutadiene skeleton may bridge two metal centers by adopting three different coordination modes in the diimino or the ene-diamido formulation. The bonding mode $\mu\text{-}\eta^2\text{-(N, N')}, \eta^2\text{-(N, N')}$, **I**, is exclusively found when the bridge is an ene-diamido $\text{C}_6\text{H}_4(\text{NR})_2\text{-}o$ ligand (aryl backbone), which behaves as eight electron donor to a $d^7\text{-}d^7 \text{L}_3\text{M-ML}_3$ system. The HOMO is essentially centered at the $\text{C}_6\text{H}_4(\text{NR})_2\text{-}o$ ligand. In absence of the phenylene ring the diazabutadiene skeleton acts as diimino bridge with two possible bonding modes, namely $\mu\text{-}\eta^2\text{-(N, N')}, \eta^2\text{-(N, C)}$, **II**, and $\mu\text{-}\eta^2\text{-(N, N')}, \eta^4\text{-(N, N', C, C')}$, **III**. In these modes the bridge behaves as six and eight electron donor ligand, respectively. In particular, the arrangement of type **II** is only observed for diimino ligands without the aryl backbone. In this case, the ligand has sufficient freedom to twist at the C–C linkage. The same torsion is more difficult for a phenyl ring, which would lose aromaticity. Concerning the $\text{C}_6\text{H}_4(\text{NR})_2\text{-}o$ ligand, the conversion of ene-diamido to diimino is chemically possible through a two electron oxidation process [20], which changes the coordination mode of the bridge from **I** to **III**. The chemical conversion of compounds $[\text{Ru}_2(\text{R,R}'\text{-DAD})(\text{CO})_6]$ into $[\text{Ru}_2(\text{R,R}'\text{-DAD})(\mu\text{-CO})(\text{CO})_4]$ derivatives by CO dissociation and the energetics associated to this process are also analyzed. The removal of a two electron donor induces the reorganization of the bridge from the coordination type **II** toward the bonding of type **III**. In this manner, the bridge is enabled to donate an additional electron pair

Table 9

Comparison of the computed model compound $[\text{Ru}_2(\mu\text{-C}_6\text{H}_4(\text{NH})_2\text{-}o)(\text{CO})_6]$, **2a**, with experimental $[\text{Ru}_2\{\mu\text{-C}_6\text{H}_4(\text{NH})_2\text{-}o\}\text{-}(\text{PPh}_3)_2(\text{CO})_4]$ complexes

Bond distances (Å) and angles (°)	Calculated 2a	Experimental	
		JETPED	JETPIH
Ru–Ru	2.613	2.558(1)	2.560(1)
Ru–N	2.177	2.167(8)	2.163(2)
	2.178	2.149(8)	2.161(2)
Ru–CO(up)	1.977	–	–
	1.978	–	–
Ru–CO(down)	1.922	1.87(1)	1.866(3)
		1.85(1)	1.858(3)
N–C	1.427	1.44(1)	1.419(4)
		1.42(1)	1.431(4)
C–C	1.410	1.41(1)	1.403(5)
Ru–N–Ru	73.7	73.1	72.6
		72.3	72.6
C–C–N	111.3	111.9	111.5
		110.7	111.0
Ru–Ru–CO(up)	148.4	–	–
CO(down)–Ru–CO(down)	91.6	91.4(5)	89.7(1)
CO(down)–Ru–CO(up)	97.2	–	–

Table 10

Computed bond distances (Å) and angles (°) for model compound $[\text{Ru}_2(\text{DAD})(\text{CO})_6]$, **2c**

Ru–Ru	2.819
Ru1–N	2.130
	2.142
Ru2–N	2.105
Ru2–C	2.252
N–C (bonded)	1.415
N–C (non bonded)	1.303
C–C	1.429
Ru1–CO(up)	1.976
Ru2–CO(up)	1.950
Ru1–CO(down)	1.930
	1.923
Ru2–CO(down)	1.925
	1.950
Ru–N–Ru	83.5
Ru–Ru–CO(up)	154.7
	156.7
C–C–N	117.1
	119.5
H–C–C–H	17.4

to the binuclear moiety and, most importantly, allows metal backdonation into a suited π^* level. This causes weakening but not disappearance of the metal–metal bond.

4. Computational details

The electronic structure and geometries of the model complexes were computed within the density functional theory at the B3LYP [49,50] level using the LANL2DZ [51,52] basis set for the iron and ruthenium atoms. The basis set used for the remaining atoms was 6-31G + (d, p). All the optimized geometries were characterized as local energy minima by diagonalization of the analytically computed Hessian (vibrational frequencies calculations). The computed IR spectra were scaled by a factor of 0.96 [53,54]. The DFT calculations were performed using the Gaussian 98 suite of programs [55]. Molecular orbitals were visualized using the GaussView program [56]. Cartesian coordinates for the optimized molecules are available from the authors upon request. The FMO analyses were done with CACAO [57] using the coordinates of the optimized model complexes.

5. Supplementary material available

Tables 9 and 10 contain bond distances and angles of the computed model compounds **2a** and **2c**, respectively.

Acknowledgments

This paper is the result of a sabbatical at ICCOM (Firenze, Italy) with financial support from the Spanish Secretaría de Estado de Educación y Universidades. My gratitude to Professor Carlo Mealli, who was a kind host and an excellent guide through the ‘forest’ of theoretical chemistry. I would like to thank to Dr. Ienco and Mr. Masi, from the same group, for their hospitality. My thanks also to all the people in the Italian Institute. Finally, I am indebted to my colleagues of our research group for allowing me to spend one year away.

References

- [1] A. Galindo, A. Ienco, C. Mealli, *New J. Chem.* 24 (2000) 73.
- [2] A. Galindo, M. Gómez, D. del Río, F. Sánchez, *Eur. J. Inorg. Chem.* (2002) 1326.
- [3] D. del Río, A. Galindo, *J. Organomet. Chem.* 655 (2002) 16.

- [4] A. Galindo, D. del Río, C. Mealli, A. Ienco, C. Bo, J. Organomet. Chem. 689 (2004) 2847.
- [5] A. Galindo, A. Ienco, C. Mealli, Comments Inorg. Chem. 23 (2002) 401.
- [6] A. Anillo, S. Garcia-Granda, R. Obeso-Rosete, A. Galindo, A. Ienco, C. Mealli, Inorg. Chim. Acta 350 (2003) 557.
- [7] F. Stoffelbach, B. Rebière, R. Poli, Eur. J. Inorg. Chem. (2004) 726.
- [8] S. Záliš, M. Sieger, S. Greulich, H. Stoll, W. Kaim, Inorg. Chem. 42 (2003) 5185.
- [9] M. Sieger, M. Wanner, W. Kaim, D.J. Stufkens, T.L. Snoeck, S. Záliš, Inorg. Chem. 42 (2003) 3340.
- [10] S. Záliš, I.R. Farrell, A. Vlček Jr., J. Am. Chem. Soc. 125 (2003) 4580.
- [11] W. Imhof, E. Anders, A. Göbel, H. Görls, Chem. Eur. J. 9 (2003) 1166.
- [12] A. Vlček Jr., Coord. Chem. Rev. 230 (2002) 225.
- [13] M. Turki, C. Daniel, Coord. Chem. Rev. 216–217 (2001) 31.
- [14] M. Turki, C. Daniel, S. Záliš, A. Vlček Jr., J. Van Slageren, D.J. Stufkens, J. Am. Chem. Soc. 123 (2001) 11431.
- [15] M.P. Aarnts, M.P. Wilms, K. Peelen, J. Fraanje, K. Goubitz, F. Hartl, D.J. Stufkens, E.J. Baerends, A. Vlček Jr., Inorg. Chem. 35 (1996) 5468.
- [16] S. Greulich, W. Kaim, A.F. Stange, H. Stoll, J. Fiedler, S. Záliš, Inorg. Chem. 35 (1996) 3998.
- [17] M. Casarin, A. Vittadini, K. Vrieze, F. Muller, G. Granozzi, R. Bertocello, J. Am. Chem. Soc. 110 (1988) 1775.
- [18] K. Vrieze, J. Organomet. Chemistry 300 (1986) 307.
- [19] G. van Koten, K. Vrieze, Adv. Organomet. Chem. 21 (1982) 151.
- [20] A. Anillo, M.R. Díaz, S. García-Granda, R. Obeso-Rosete, A. Galindo, A. Ienco, C. Mealli, Organometallics 23 (2004) 471.
- [21] J. Keijsper, L.H. Polm, G. van Koten, K. Vrieze, P.F.A.B. Seignette, C.H. Stam, Inorg. Chem. 24 (1985) 518.
- [22] J. Keijsper, L.H. Polm, G. van Koten, K. Vrieze, K. Goubitz, C.H. Stam, Organometallics 4 (1985) 1876 and 2006.
- [23] L.H. Staal, L.H. Polm, K. Vrieze, F. Ploeger, C.H. Stam, Inorg. Chem. 20 (1981) 3590.
- [24] R. Zoet, G. van Koten, D.J. Stufkens, K. Vrieze, C.H. Stam, Organometallics 7 (1988) 2118.
- [25] Cambridge Structural Database System, Cambridge Crystallographic data Centre, 12 Union Road, Cambridge, CB2 1EZ, UK. F.H. Allen, O. Kennard, Chem. Des. Autom. News 8 (1993) 31.
- [26] S. Garcia-Granda, R. Obeso-Rosete, J.M. Rubio, A. Anillo, Acta Crystallogr. Sect. C 46 (1990) 2043.
- [27] P.E. Baikie, O.S. Mills, Inorg. Chim. Acta 1 (1967) 55.
- [28] H. Kisch, P. Reisser, F. Knoch, Chem. Ber. 124 (1991) 1143.
- [29] A. Anillo, R. Obeso-Rosete, M.A. Pellinghelli, A. Tiripicchio, J. Chem. Soc., Dalton Trans. (1991) 2019.
- [30] W. Imhof, A. Göbel, R. Beckert, T. Billert, H. Görls, J. Organomet. Chem. 590 (1999) 104.
- [31] R. Zoet, G. Van Koten, F. Muller, K. Vrieze, M. Van Wijnkoop, K. Goubitz, C.J.G. Van Halen, C.H. Stam, Inorg. Chim. Acta 149 (1988) 193.
- [32] H.-W. Fruhauf, A. Landers, R. Goddard, C. Kruger, Angew. Chem. Int. Ed. Engl. 17 (1978) 64.
- [33] P.L. Motz, J.P. Williams, J.J. Alexander, D.M. Ho, J.S. Ricci, W.T. Miller Jr., Organometallics 8 (1989) 1523.
- [34] R.D. Adams, J. Am. Chem. Soc. 102 (1980) 7476.
- [35] L.H. Staal, L.H. Polm, R.W. Balk, G. Van Koten, K. Vrieze, A.M.F. Brouwers, Inorg. Chem. 19 (1980) 3343.
- [36] R. Zoet, G. Van Koten, A.L.J. Van der Panne, P. Versloot, K. Vrieze, C.H. Stam, Inorg. Chim. Acta 149 (1988) 177.
- [37] L.H. Staal, J. Keijsper, G. Van Koten, K. Vrieze, J.A. Cras, W.P. Bosman, Inorg. Chem. 20 (1981) 555.
- [38] M.J.A. Kraakman, C.J. Elsevier, V.W. de Haar, K. Vries, A.L. Spek, Inorg. Chim. Acta 203 (1993) 157.
- [39] M.J.A. Kraakman, K. Vrieze, H. Kooijman, A.L. Spek, Organometallics 11 (1992) 3760.
- [40] J. Keijsper, L. Polm, G. Van Koten, K. Vrieze, G. Abbell, C.H. Stam, Inorg. Chem. 23 (1984) 2142.
- [41] L.H. Staal, G. Van Koten, K. Vrieze, F. Ploeger, C.H. Stam, Inorg. Chem. 20 (1981) 1830.
- [42] F. Muller, G. Van Koten, K. Vrieze, D. Heijdenrijk, Inorg. Chim. Acta 158 (1989) 69.
- [43] F. Muller, G. Van Koten, M.J.A. Kraakman, K. Vrieze, R. Zoet, K.A.A. Duineveld, D. Heijdenrijk, C.H. Stam, M.C. Zoutberg, Organometallics 8 (1989) 982.
- [44] C. Mealli, A. Ienco, A. Anillo, S. Garcia-Granda, R. Obeso-Rosete, Inorg. Chem. 36 (1997) 3724.
- [45] For a recent paper devoted to the theoretical analysis of binuclear manganese complexes containing a metal–metal bond, see: Y. Xie, J.H. Jang, R.B. King, H.F. Schaefer III, Inorg. Chem. 42 (2003) 5219.
- [46] T.A. Albright, J.K. Burdett, M.-H. Whangbo, Orbital Interactions in Chemistry, Wiley, New York, 1985.
- [47] For an example of a new approach to the study of M–M bonds, see: M. Finger, J. Reinhold, Inorg. Chem. 42 (2003) 8128.
- [48] S. Petrie, R. Stranger, Inorg. Chem. 43 (2004) 2597.
- [49] A.D. Becke, J. Chem. Phys. 98 (1993) 5648.
- [50] C. Lee, W. Yang, R.G. Parr, Phys. Rev. B 37 (1988) 785.
- [51] T.H. Dunning Jr., P.J. Hay, in: Modern Theoretical Chemistry, Plenum, New York, 1976, p. 1.
- [52] P.J. Hay, W.R. Wadt, J. Chem. Phys. 82 (1985) 299.
- [53] W. Wong, Chem. Phys. Lett. 256 (1996) 391.
- [54] A.P. Scott, L. Radom, J. Phys. Chem. 100 (1996) 16502.
- [55] M.J. Frisch, G.W. Trucks, H.B. Schlegel, G.E. Scuseria, M.A. Robb, J.R. Cheeseman, V.G. Zakrzewski, J.A. Montgomery Jr., R.E. Stratmann, J.C. Burant, S. Dapprich, J.M. Millam, A.D. Daniels, K.N. Kudin, M.C. Strain, O. Farkas, J. Tomasi, V. Barone, M. Cossi, R. Cammi, B. Mennucci, C. Pomelli, C. Adamo, S. Clifford, J. Ochterski, G.A. Petersson, P.Y. Ayala, Q. Cui, K. Morokuma, D.K. Malick, A.D. Rabuck, K. Raghavachari, J.B. Foresman, J. Cioslowski, J.V. Ortiz, A.G. Baboul, B.B. Stefanov, G. Liu, A. Liashenko, P. Piskorz, I. Komaromi, R. Gomperts, R.L. Martin, D.J. Fox, T. Keith, M.A. Al-Laham, C.Y. Peng, A. Nanayakkara, C. Gonzalez, M. Challacombe, P.M.W. Gill, B. Johnson, W. Chen, M.W. Wong, J.L. Andres, M. Head-Gordon, E.S. Replogle, J.A. Pople, Gaussian 98, Revision A.7, Gaussian, Inc., Pittsburgh, PA, 1998.
- [56] GaussView 2.08, Gaussian, Inc., Pittsburgh, PA, USA.
- [57] C. Mealli, D.M. Proserpio, J. Chem. Educ. 67 (1990) 399.